JOURNAL OF BACTERIOLOGY, Mar. 2010, p. 1685–1699 Vol. 192, No. 6
0021-9193/10/$12.00 doi:10.1128/JB.01518-09

Genome Sequence of the Deep-Rooted *Yersinia pestis* Strain Angola Reveals New Insights into the Evolution and Pangenome of the Plague Bacterium▽†

Mark Eppinger,[1] Patricia L. Worsham,[2] Mikeljon P. Nikolich,[3] David R. Riley,[1] Yinong Sebastian,[4] Sherry Mou,[2] Mark Achtman,[5] Luther E. Lindler,[6] and Jacques Ravel[1]*

Institute for Genome Sciences (IGS) and Department of Microbiology and Immunology, University of Maryland, School of Medicine, Baltimore, Maryland 21201[1]; U.S. Army Medical Research Institute of Infectious Diseases (USAMRIID), Bacteriology Division, Fort Detrick, Maryland 21702[2]; Walter Reed Army Institute of Research (WRAIR), Division of Bacterial & Rickettsial Diseases, Silver Spring, Maryland 20910[3]; J. Craig Venter Institute, Rockville, Maryland 20850[4]; Environmental Research Institute (ERI), University College Cork, Lee Road, Cork, Ireland[5]; and Department of Defense, Global Emerging Infections Surveillance and Response System, 503 Robert Grant Ave., Silver Spring, Maryland 20910[6]

Received 20 November 2009/Accepted 25 December 2009

To gain insights into the origin and genome evolution of the plague bacterium *Yersinia pestis*, we have sequenced the deep-rooted strain Angola, a virulent Pestoides isolate. Its ancient nature makes this atypical isolate of particular importance in understanding the evolution of plague pathogenicity. Its chromosome features a unique genetic make-up intermediate between modern *Y. pestis* isolates and its evolutionary ancestor, *Y. pseudotuberculosis*. Our genotypic and phenotypic analyses led us to conclude that Angola belongs to one of the most ancient *Y. pestis* lineages thus far sequenced. The mobilome carries the first reported chimeric plasmid combining the two species-specific virulence plasmids. Genomic findings were validated in virulence assays demonstrating that its pathogenic potential is distinct from modern *Y. pestis* isolates. Human infection with this particular isolate would not be diagnosed by the standard clinical tests, as Angola lacks the plasmid-borne capsule, and a possible emergence of this genotype raises major public health concerns. To assess the genomic plasticity in *Y. pestis*, we investigated the global gene reservoir and estimated the pangenome at 4,844 unique protein-coding genes. As shown by the genomic analysis of this evolutionary key isolate, we found that the genomic plasticity within *Y. pestis* clearly was not as limited as previously thought, which is strengthened by the detection of the largest number of isolate-specific single-nucleotide polymorphisms (SNPs) currently reported in the species. This study identified numerous novel genetic signatures, some of which seem to be intimately associated with plague virulence. These markers are valuable in the development of a robust typing system critical for forensic, diagnostic, and epidemiological studies.

Yersinia pestis, the causative agent of plague, is a nonmotile Gram-negative bacterial pathogen. The genus *Yersinia* comprises two other pathogens that cause worldwide infections in humans and animals: *Y. pseudotuberculosis* and *Y. enterocolitica* (11, 12, 22, 61, 71). Despite their genetic relationship, these species differ radically in their pathogenicity and transmission. Plague is primarily a disease of wild rodents that is transmitted to other mammals through flea bites. In humans it produces the bubonic form of plague. *Y. pestis* also can be transmitted from human to human by aerosol, especially during pandemics, causing primarily pneumonic plague. Evolutionarily, it is estimated that *Y. pestis* diverged from the enteric pathogen *Y. pseudotuberculosis* within the last 20,000 years, while *Y. pseudotuberculosis* and *Y. enterocolitica* lineages separated 0.4 to 1.9 million years ago (2). *Y. pestis* inhabits a distinct ecological niche, and its transmission is anchored in its unique plasmid inventory: the murine toxin (pMT) and plasminogen activator (pPCP) plasmids. In addition, *Y. pestis* harbors the low-calcium-response plasmid pCD, which it inherited from its closest relative, *Y. pseudotuberculosis* (pYV) (12), and it also is found in the more distantly related *Y. enterocolitica* (71). So-called cryptic plasmids have been described in the literature as part of the *Y. pestis* mobilome (71), but no sequence data are available to decipher the nature and impact of such plasmids in the epidemiology and pathogenicity of *Y. pestis* (14). *Y. pestis* isolates have been historically grouped into the biovars Antiqua (ANT), Medievalis (MED), and Orientalis (ORI), based on metabolic properties such as nitrate reduction and fermentation patterns (72). However, we will use the population-based nomenclature for *Y. pestis* introduced by Achtman et al. (1), as we believe it better reflects the true evolutionary relationship. Due to its young evolutionary age, only a few genetic polymorphisms have been identified within the *Y. pestis* genomes sequenced to date (1). Here, we report the comparative analysis of the virulent *Y. pestis* strain Angola, a representative of one of the most ancient *Y. pestis* lineages thus far sequenced. We studied adaptive microevolutionary traits *Y. pestis* has acquired and predicted the global *Yersinia* pangenome. By comparing the genomes of the three human pathogenic *Yersinia* species

* Corresponding author. Mailing address: Institute for Genome Sciences, University of Maryland School of Medicine, 801 W. Baltimore St., Baltimore, MD 21201. Phone: (410) 706-5674. Fax: (410) 706-6756. E-mail: jravel@som.umaryland.edu.

† Supplemental material for this article may be found at http://jb.asm.org/.

▽ Published ahead of print on 8 January 2010.

(12, 22), we investigated the global- and species-specific gene reservoir, the genome dynamics, and the degree of genetic diversity that is found within these species. Our genotypic and phenotypic analyses, as well as the refined single-nucleotide polymorphism (SNP)-based phylogeny of *Y. pestis*, indicate that Angola is a deep-rooted isolate with unique genome characteristics intermediate between modern *Y. pestis* isolates and *Y. pseudotuberculosis*.

MATERIALS AND METHODS

Biological material. *Y. pestis* strain Angola was grown from a lyophilized stock prepared in 1984 at the U.S. Army Medical Institute for Infectious Diseases. Since then, the primary glycerol stock was passed in the laboratory only once for the purpose of this sequencing project. Strains CO92 and Pestoides A and F were used in the mutator assay. Female Swiss Webster mice, BALB/c mice, and Hartley guinea pigs were used to assess the virulence of strain Angola.

Genome sequencing, annotation, and analysis. Genomic DNA of *Y. pestis* strain Angola was subjected to random shotgun sequencing and closure strategies as previously described (22). Random insert libraries of 3 to 5 kb and 10 to 12 kb were constructed, and 61,634 high-quality sequences of an 837-nt average read length were obtained. Draft genome sequences were assembled using the Celera assembler (38). The chromosome and the three plasmids were manually annotated using MANATEE (http://manatee.sourceforge.net/). To obtain copy numbers for the plasmids, their sequence coverage was calculated and normalized to the chromosome sequence coverage.

Comparative genomics and genome visualization. The whole-genome alignment tool MUMmer (42) was used to calculate the overall gene identities of strain Angola to the *Y. pestis*, *Y. pseudotuberculosis*, and *Y. enterocolitica* genomes. Each of the predicted genes of strain Angola was classified as conserved, shared, and unique according to the computed BLAST score ratio values and nucleotide identities. For each of the predicted proteins of *Y. pestis* Angola, a BLASTP raw score was obtained for the alignment against itself (REF_SCORE) and the most similar protein (QUE_SCORE) in each of the genomes of *Y. pestis*, *Y. pseudotuberculosis*, and *Y. enterocolitica*. Dividing the QUE_SCORE obtained for each query genome protein by the REF_SCORE normalized these scores and constitutes the blast score ratio (BSR). Proteins with a normalized BSR of <0.4 were considered nonhomologous. A normalized BSR of 0.4 corresponded to two proteins being 30% identical over their entire length (56). Proteins with a normalized BSR of <0.4 were considered nonhomologous. A normalized BSR of 0.4 corresponded to two proteins being 30% identical over their entire length (56). The chi-squared values and G+C skews were computed from the Angola molecules as previously described (22, 51). For the chromosomal chi-square test, a window size of 2 kb and a sliding window of 1 kb were used, while a window size of 1 kb and a sliding window of 0.2 kb were used for the two plasmids. G+C skews were calculated using the software gcskew with a window size of 1 kb for the chromosome and 0.2 kb for the plasmids.

Rodent virulence studies. (i) LD_{50} determination in Swiss Webster mice. To prepare inocula for aerosol and subcutaneous challenges, samples from frozen stocks were streaked on tryptose blood agar base slants and incubated at 28°C for 48 h. For the aerosol challenge, slants were flushed with heart infusion broth containing 0.2% xylose. The sample was adjusted to an A_{620} of 1.0, and 1 ml of this suspension was added to 100 ml of HIB-xylose (6). The liquid culture was incubated in a rotating shaker (150 rpm) in tightly capped flasks for 24 h at 30°C. Bacterial cells were pelleted and resuspended in heart infusion broth (HIB) (no added xylose). For aerosol exposure, starting concentrations were prepared as 10-fold serial dilutions from the highest dose. Mice (5 to 7 weeks old) were exposed using an ~1-μm-generating Collison nebulizer contained within a class III biocabinet in a temperature- and humidity-controlled whole-body exposure chamber. The aerosol was continuously sampled by an all-glass impinger (AGI) containing HIB. The inhaled dose was determined from the serial dilution and culture of AGI samples according to the formula determined by Guyton (32). Samples of the starting material for aerosol exposures were diluted and spread on sheep blood agar plates (SBAP) to obtain the starting concentration. Samples collected in the AGIs were diluted and spread on SBAP. For the subcutaneous challenge, slants were flushed with 10 mM potassium phosphate buffer (pH 7.0) and diluted to the desired concentration. Samples of the starting material were diluted and spread on SBAP plates to obtain the number of organisms administered to the animals. Animals were observed twice daily for at least 21 days postexposure, and 50% lethal dose (LD_{50}) values were determined by probit analysis. For both aerosol and subcutaneous challenges, the LD_{50} studies included five groups of 10 animals each. The starting concentrations for the subcutaneous challenges were prepared as 10-fold serial dilutions from the highest dose. Mice were challenged subcutaneously between the scapulae with 200 ml of *Y. pestis* suspended in 10 mM potassium phosphate buffer (pH 7). Animals were observed twice daily for at least 21 days postexposure. LD_{50} values were determined by probit analysis.

(ii) Virulence in BALB/c mice and Hartley guinea pigs models. The comparison of virulence in mice (20 g, 6 weeks old) and guinea pigs (0.8 to 1 kg) was done via the intradermal route of infection using strain Angola versus a control strain of typical *Y. pestis* CO92. The strains were introduced in suspensions using tuberculin syringes with 25- to 27-gauge needles with injection into the dermal layer of the skin (skin bubble). Each strain was delivered at the two doses of 1×10^2 and 1×10^6 CFU of each strain. Bacterial cells for injection were made by diluting suspensions from fresh slants. Animals were tested in groups of six. The animals were observed daily at 4-h intervals for 2 weeks. Relative virulence was determined by lethality and mean time to death for each dose.

Comparative mutational analysis. Ten colonies of each *Y. pestis* strain analyzed were tested for spontaneous nalidixic acid resistance. Ten isolated colonies of each *Y. pestis* strain tested were grown in tubes containing 10 ml brain heart infusion (BHI) broth for 48 h at 28°C with shaking at 200 rpm. The A_{600} then was determined for each culture. For each bacterial suspension, a volume of 0.2 ml was streaked onto two BHI agar plates (50) containing nalidixic acid (100 μg/ml). The number of colonies on each plate was counted after incubation for 48 h at 28°C. The proportion of spontaneous resistance in the bacterial population was calculated for each tested strain as follows: mutation rate = (number of resistant colonies)(5)/$(1.75 \times 10^9)(A_{600}$ reading). The number of bacterial cells in one A_{600} unit is approximately 1.75×10^9 CFU/ml. The average of 10 mutation rate determinations then was calculated to arrive at the overall mutation rate for each strain.

Single-nucleotide polymorphism discovery. Single-nucleotide polymorphisms were identified in pairwise genome comparisons by comparing the predicted genes on the closed chromosome of *Y. pestis* strain CO92 to the completed genomes of strains KIM, Antiqua, Nepal516, 9001, and Pestoides F using MUMmer (19), and draft contigs were used for strains CA88-4125 (8) and FV-1 (63). By mapping the position of the SNP to the annotation in the reference strain CO92 genome, it was possible to determine the effect on the deduced polypeptide and classify each SNP as synonymous or nonsynonymous. For genomes with deposited underlying sequencing information, a polymorphic site was considered of high quality when it was represented by three underlying sequence reads with an average Phred quality score of greater than 30 (23). The SNP data set was manually curated, and positions within repeats and lateral acquired genomic regions were excluded from the phylogenetic analysis.

Phylogenetic analyses. SNP data were analyzed further using the HKY93 algorithm (35) with 500 bootstrap replicates, and a phylogenetic tree was constructed using the PhyML algorithms (30). The Geneious software package (http://www.geneious.com) and SplitsTree4 (37) were used for visualization.

Core genes and gene discovery computation. To compute the core gene, new gene, and pangenome estimates, all-versus-all WU-BLASTP and all-versus-all WU-TBLASTN were performed according to W. Gish (http://blast.wustl.edu) (5). The results from these two searches were combined such that the TBLASTN prevented missing gene annotations from producing false negatives. Hits were filtered such that homologues were defined as having 50% sequence similarity over at least 50% of the length of the protein.

Pangenome computation. To compute core gene, new gene, and pangenome estimates, all-versus-all WU-BLASTP and -TBLASTN were performed (5). The determination of core genes and strain-specific genes depends on the number of genomes included in the analysis. The number (N) of independent measurements of the core and strain-specific genes present in the n^{th} genome is $N = S/\{(n-1)! \cdot (S-n)!\}$, where S is 14 (*Y. pestis*), 16 (*Y. pestis* and *Y. pseudotuberculosis*), and 17 (*Y. pestis* and *Y. pseudotuberculosis* and *Y. enterocolitica*). A random sampling of 1,000 measurements for each value of n was calculated to reduce the number of required computations. The numbers of core and strain-specific genes for a large number of sequenced isolates were extrapolated by fitting the exponential decaying functions $F_c(n) = \kappa_c \exp[-n/\tau_c] + tg_c(\theta)$ and $F_n(n) = \kappa_n \exp[-n/\tau_n] + tg_n(\theta)$, respectively, to the mean number of conserved and strain-specific genes calculated for all strain combinations. n is the number of sequenced strains, and κ_c, τ_c, κ_n, τ_n, $tg_c(\theta)$, and $tg_n(\theta)$ are free parameters. $tg_c(\theta)$ and $tg_n(\theta)$ represent the extrapolated number of core and strain-specific genes, assuming a consistent sampling mechanism and a large number of completed sequences. The pangenome itself represents an estimation of the complete gene pool based on the set of genomes analyzed and was computed in triplicates. In this case, a sample of at most 1,000 combinations for each value of n was taken and the total number of genes, both shared and strain specific, was

TABLE 1. Genomic features of *Y. pestis* Angola

Genomic element	Molecule		Open reading frame			No. of noncoding RNAs	
	Genome size (bp)	GC content (%)	Predicted no.	Coding area (%)	Avg length (bp)	rRNA	tRNA
Chromosome	4,504,290	47.5	4,255	82.7	879	20	70
pCD	68,190	44.7	105	79.2	514	0	0
pMT-PCP	114,570	50	145	84.6	668	0	0
pPCP	9,608	45.2	19	78.2	395	0	0

calculated. To estimate the total number of genes accessible to the subsets of tested genomes or the pangenome, the median values at each *n* then were fitted with an exponential decay function as the core and new gene graphs.

Synteny analysis. To study the genome dynamics, paralog clusters in each genome were computed by using the Jaccard algorithm according to reference 39 by applying a Jaccard coefficient of 0.6 and an 80% identity threshold. Members of paralog clusters then were organized into ortholog clusters by allowing any member of a paralog cluster to contribute to the reciprocal best matches used to construct the ortholog clusters. The presence or absence of a gene from the reference strain Angola in a query genome was determined based on whether the query genome had a member in the reference gene's ortholog cluster. Query gene matches are drawn above their reference gene hits and are colored based on the position in the query genome. Genes colored black indicate that there are multiple clusters in the reference genome. The gradient display was drawn using these ortholog clusters with the SYBIL software package (http://sybil.sourceforge.net/).

Nucleotide sequence accession numbers. The *Y. pestis* Angola genome sequence (Project 16067) has been deposited under GenBank accession nos. CP000901 (chromosome), CP000900 (pMT-PCP), and CP000902 (pCD). The respective genome assemblies have been deposited in the NCBI Assembly Archive under ID3452 with an average coverage of 11.54×, and the 67,293 sequencing traces are available from the NCBI Trace Archive.

RESULTS

Genome architecture. The chromosome of *Y. pestis* Angola consists of a circular molecule of 4,504,290 bp, with an average G+C content of 47.5% (Table 1, Fig. 1A). No well-defined G+C bias was observed, which is indicative of recent and frequent intrachromosomal recombinatorial events. The Angola mobile genome pool comprises the 69,190-bp pCD plasmid and a larger 114,570-bp chimeric plasmid, designated pMT-PCP, not previously seen in *Y. pestis*, which is composed of the murine toxin plasmid and two tandemly inserted copies of the plasminogen activator plasmid (Fig. 1B). The plasmid profile of strain Angola reveals the presence of an autonomous pPCP plasmid that replicates independently of the chimeric version and clearly shows the increased size of pMT-PCP compared to that of a typical pMT plasmid of strain CO92 (see Fig. S1 in the supplemental material). Gene dosage effects might be involved in pMT-PCP-borne pathogenicity, as the copy number of the chimeric plasmid is increased compared to that of isolates with a standard plasmid inventory. We estimated the strain Angola plasmid copy numbers by comparing the average plasmid sequence coverage to that of the chromosome with two pCD and four pMT-pPCP copies per chromosome for strain Angola, and the pMT-PCP plasmid clearly features the higher pPCP copy number under identical cultivation conditions. Thus, this chimeric plasmid appears to be under the replication control of pPCP, and its unique architecture might result in potential dosage effects of not only pPCP-borne but also pMT-borne virulence determinants.

Genome dynamics and gene inventory. To study the Angola genome architecture, we investigated the population-wide genome dynamics among the seven closed *Y. pestis* genomes. The comprehensive intra- and interspecies analysis of the virulence plasmid and the chromosome architecture (see Fig. S2 in the supplemental material) reveals a high degree of intrachromosomal rearrangements in strain Angola, a characteristic feature of the *Y. pestis* genome evolution (17). The amino acid similarities show only marginal deviations within the analyzed *Y. pestis* isolates, and no obvious correlations between the traditional biovar classification and the degree of proteome conservation were detected (see Table S1 in the supplemental material), confirming the disconnect observed by Achtman et al. (1) between the biovar nomenclature and *Y. pestis* evolution. The species borders are clearly reflected in the interspecies comparisons of the Angola proteome to its closest phylogenetic neighbor, *Y. pseudotuberculosis* (12, 22), and to the more distantly related pathogen *Y. enterocolitica* (61). The chromosomes display only local microsynteny but no genome-wide synteny, and both the murine toxin plasmid pMT (see Fig. S2A in the supplemental material) and low-calcium-response plasmid pCD (pYV) (see Fig. S2B) feature multiple intraplasmid rearrangements. In contrast to these molecules, the organization of the *Y. pestis*-specific plasmid pPCP is highly syntenic. These observed rearrangements are associated with a massive expansion of insertion sequence (IS) elements and clearly distinguish strain Angola from its phylogenetic progenitor, *Y. pseudotuberculosis* (12, 22) (Fig. 1A). A similar role of IS element expansion in chromosomal reorganization has been implicated in the genome evolution and pathogenicity of *Bordetella* species (16). Besides the abundance of IS elements in strain Angola, we also observed isolate-specific propagation patterns of the four IS element types within *Y. pestis* that drive not only the reorganization of their genomic architecture (62) but also the microevolution of the metabolic capabilities (59) (see Fig. S3 in the supplemental material).

Ancestral metabolic capabilities and biovar designation. Strain Angola is capable of fermenting glycerol and reducing nitrate and would be biochemically classified as a biovar ANT isolate (72). The nitrate reductase gene, *napA* (YpAngola_A2791), is identical to that of other *Y. pestis* nitrate reducers, while a new polymorphic state, an alanine-to-serine alteration at position 175 that is unique to Angola (GCA->TCA), was found in *glpD* (YpAngola_A4123), a glycerol-3-phosphate dehydrogenase that is key to the identification of the glycerol fermentation phenotype.

Angola is further associated with the Pestoides group originating in central Asia (7, 27, 59), because it can metabolize

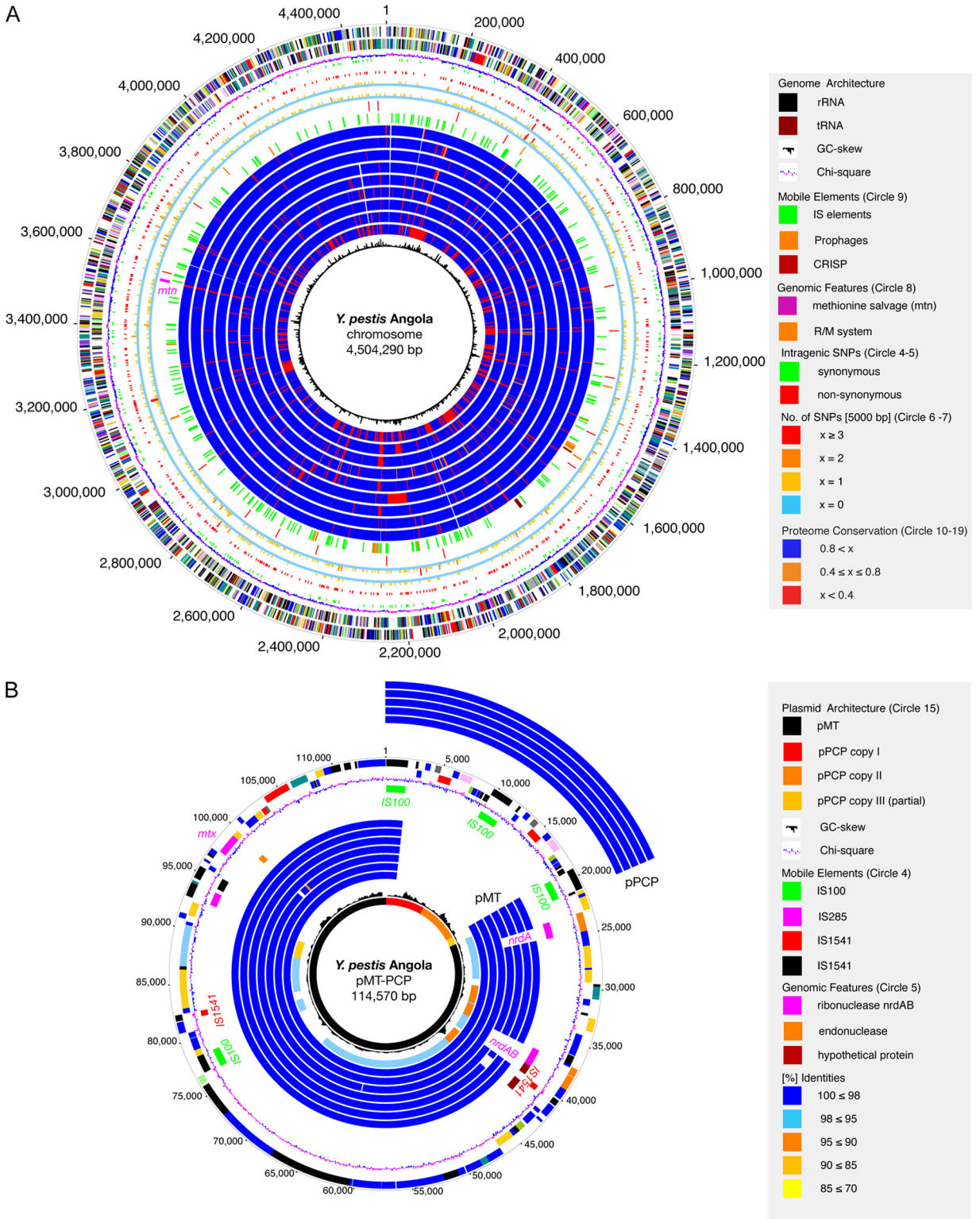
A
1
200,000
400,000
600,000
800,000
1,000,000
1,200,000
1,400,000
1,600,000
1,800,000
2,000,000
2,200,000
2,400,000
2,600,000
2,800,000
3,000,000
3,200,000
3,400,000
3,600,000
3,800,000
4,000,000
4,200,000
4,400,000
mtn
Y. pestis Angola
chromosome
4,504,290 bp
Genome Architecture
rRNA
tRNA
GC-skew
Chi-square
Mobile Elements (Circle 9)
IS elements
Prophages
CRISP
Genomic Features (Circle 8)
methionine salvage (mtn)
R/M system
Intragenic SNPs (Circle 4-5)
synonymous
non-synonymous
No. of SNPs [5000 bp] (Circle 6 -7)
x ≥ 3
x = 2
x = 1
x = 0
Proteome Conservation (Circle 10-19)
0.8 < x
0.4 ≤ x ≤ 0.8
x < 0.4
B
1
5,000
10,000
15,000
20,000
25,000
30,000
35,000
40,000
45,000
50,000
55,000
60,000
65,000
70,000
75,000
80,000
85,000
90,000
95,000
100,000
105,000
110,000
IS100
IS100
IS100
IS100
mtx
pPCP
pMT
nrdA
nrdAB
IS1541
IS1541
IS100
Y. pestis Angola
pMT-PCP
114,570 bp
Plasmid Architecture (Circle 15)
pMT
pPCP copy I
pPCP copy II
pPCP copy III (partial)
GC-skew
Chi-square
Mobile Elements (Circle 4)
IS100
IS285
IS1541
IS1541
Genomic Features (Circle 5)
ribonuclease nrdAB
endonuclease
hypothetical protein
[%] Identities
100 ≤ 98
98 ≤ 95
95 ≤ 90
90 ≤ 85
85 ≤ 70
C
5'-pMT
pPCP copy I
pPCP copy II
copy III
1
9608
19216
Yp_139
IS100
IS21
Yp_31

melibiose (mel) and rhamnose (rha). These ancestral capabilities can be used to differentiate *Y. pestis* from *Y. pseudotuberculosis*, as well as differentiate modern *Y. pestis* isolates from those of the deep-branching Pestoides group (48). In strain Angola, the rhamnose pathway (YpAngola_0737 to YpAngola_0748) consists of the transport gene *rhaT*, two regulatory transcriptional activators, *rhaRS*, three structural genes, *rhaBAD*, the lactalaldehyde reductase *fucO* and epimerase *rhaU*, and three interspersed hypothetical genes (YpAngola_0739, YpAngola_0741, and YpAngola_0742) with no assigned function (see Fig. S4 in the supplemental material). Among the identified polymorphisms within the *rha* locus, only a single genetic polymorphism (CAC→CGC; position 671) in the transcriptional activator rhamnose RhaS was consistently observed in modern *Y. pestis* isolates (41). This regulator previously has been associated with the activation of rhamnose metabolism in *Escherichia coli* (67), and thus the observed arginine-to-histidine alteration most likely is responsible for the rhamnose-negative phenotype in modern isolates. Interestingly, unlike previous findings by Kukleva et al. (41), we detected sequence variations not only in the regulator *rhaS* but also in both structural subunits *rhaB* and *rhaD*, while all other genes were found to be genetically identical within *Y. pestis* (see Fig. S4 in the supplemental material). These differences are not consistent among rhamnose-positive or -negative isolates and thus certainly are not responsible for the conversion of the rhamnose phenotype in *Y. pestis*. However, within rhamnose-positive isolates, these genetic variations might account for observed differences in the kinetics of rhamnose metabolism (15). Further, strains Angola and Pestoides F (27) carry the methionine salvage pathway *mtnKADCEBU* (YpAngola_A3328 to YpAngola_A3333) (Fig. 2A). This salvage cycle maintains methionine levels by recycling methylthioadenosine (MTA), a product of the biosynthesis of polyamines into methionine (57). This pathway is conserved in *Y. pseudotuberculosis* serovar I strains IP31758 (22), IP32953 (12), PB1 (NC_010634), and serovar III strain YPIII (NC_010465), as well as the more distantly related *Y. enterocolitica* strain 8081 (61). The presence of these ancestral pathways in strain Angola and the progenitor *Y. pseudotuberculosis* suggests that these loci have been lost secondarily in modern *Y. pestis* but were present in the ancestral root of this lineage, thereby supporting the relationship of ancestral strain Angola to modern *Y. pestis* (Fig. 1A and 2A). This hypothesis is strengthened by the presence of a 5′-methylthioadenosine/*S*-adenosylhomocysteine nucleosidase (*mtnN*), a further component of the *mtn* pathway located elsewhere in the genome that is found in all sequenced *Y. pestis* strains (22).

Microevolution of the virulence plasmids. We investigated microevolutionary processes that might have shaped the organization of Angola virulence plasmids. The genomic analysis of strain Angola reveals a unique chimeric 114,570-bp plasmid featuring an architecture not observed in any *Y. pestis* isolates sequenced previously (Fig. 1B). Unusual sizes among the typical virulence plasmids previously were attributed to intrachromosomal deletions and the lateral acquisition of genomic fragments (28). It is noteworthy that architectural variations consisting of independently replicating pPCP dimers have been reported in strains isolated from the western United States (14). The pMT-PCP plasmid is composed of the murine toxin plasmid disrupted by two tandemly repeated copies of the pPCP plasmid. This architecture accounts for the large plasmid size and deviating G+C content in a head-to-tail arrangement (Fig. 1C). The presence of the IS*100* element (Fig. 1B) on both virulence plasmids might have facilitated the mechanistic process of cointegration via double homologous recombination, resulting in the chimeric nature of this plasmid. It is not clear if the presence of this chimeric plasmid provides any advantage to strain Angola or arose due to defects in plasmid maintenance and the replication of pMT and pPCP. Enzymatic defects cause incomplete partitioning during replication and decatenation and might result in the dimeric plasmid (14). We speculate that the unique plasmid architecture in Angola helps to guarantee a stable maintenance of both plasmids pMT and pPCP, as these two virulence plasmids are known to be unstable in *Y. pestis* (44). Indeed, other Pestoides isolates lack one of the two species-specific virulence plasmids (see Fig. S1 in the supplemental material) (9, 27), and we found the chimeric plasmid to be stable even after extensive laboratory cultivation. The plasmid profile of four Pestoides isolates shows atypically large pMT plasmids (9). However, in at least two of these strains, Pestoides F (27) and G8786 (28), the larger size is the result of additional conjugal transfer system genes and evolved independently from the Angola-specific pPCP dimer integration. The Angola genome carries three copies of the plasmid-associated plasminogen activator genes (*pla*) that help promote the dissemination of *Y. pestis* through peripheral infection routes (43). Thus, gene dosage effects of Pla virulence determinants might affect the pathogenic potential of strain Angola via endogenous plasmid control (60). The lateral acquisition of these two virulence plasmids was a key step in the *Y. pestis* speciation and contributed to its evolutionary transformation from an enteric pathogen into a highly host-adapted mammalian blood-borne pathogen. The finding of this unique

FIG. 1. (A) Circular representation of the *Y. pestis* Angola chromosome. Circles, from outer to inner: predicted open reading frames encoded on the plus (1) and minus strands (2), colored according to the respective MANATEE roles; (3) G+C skew; (4) sSNP; (5) nsSNP; (6 and 7) genome-wide distribution of SNPs; (8) chromosomal regions of interest; (9) mobile elements; (10 to 18) comparative analysis of the Angola proteome to strains CO92 (10), KIM (11), Antiqua (12), Nepal516 (13), 91001 (14), and Pestoides F (15); interspecies comparison to *Y. pseudotuberculosis* strains IP32953 (16) and IP31758 (17) and *Y. enterocolitica* 8081 (18); (19) chi-square values. (B) Chimeric plasmid pMT-PCP. Circles, from outer to inner: (1 and 2) predicted open reading frames; (3) G+C skew; (4) mobile elements. Circle fragments for comparison to the pPCP plasmid are on the outside and show *Y. pestis* strains CO92 (1), KIM (2), 91001 (3), Antiqua (4), and Nepal516 (5); circle fragments for comparison to the pMT plasmids are on the inside and show strains CO92 (6), KIM (7), 91001 (8), Antiqua (9), Nepal516 (10), Pestoides F (11), and G8787 (12); circles for interspecies comparison to *S. enterica* CT18 pHCM2 plasmid (13); (14) chi-square values; (15) chimeric plasmid composition. Plasmid regions secondarily lost in the *Y. pestis* evolution, such as ribonucleases *nrdAB* and the Nepal516-specific 1,220-bp deletion of four hypothetical proteins with no assigned function (brown). (C) Architecture of pMT-PCP. The plasmid features a pPCP dimer integrated into the pMT plasmid in a head-to-tail arrangement.

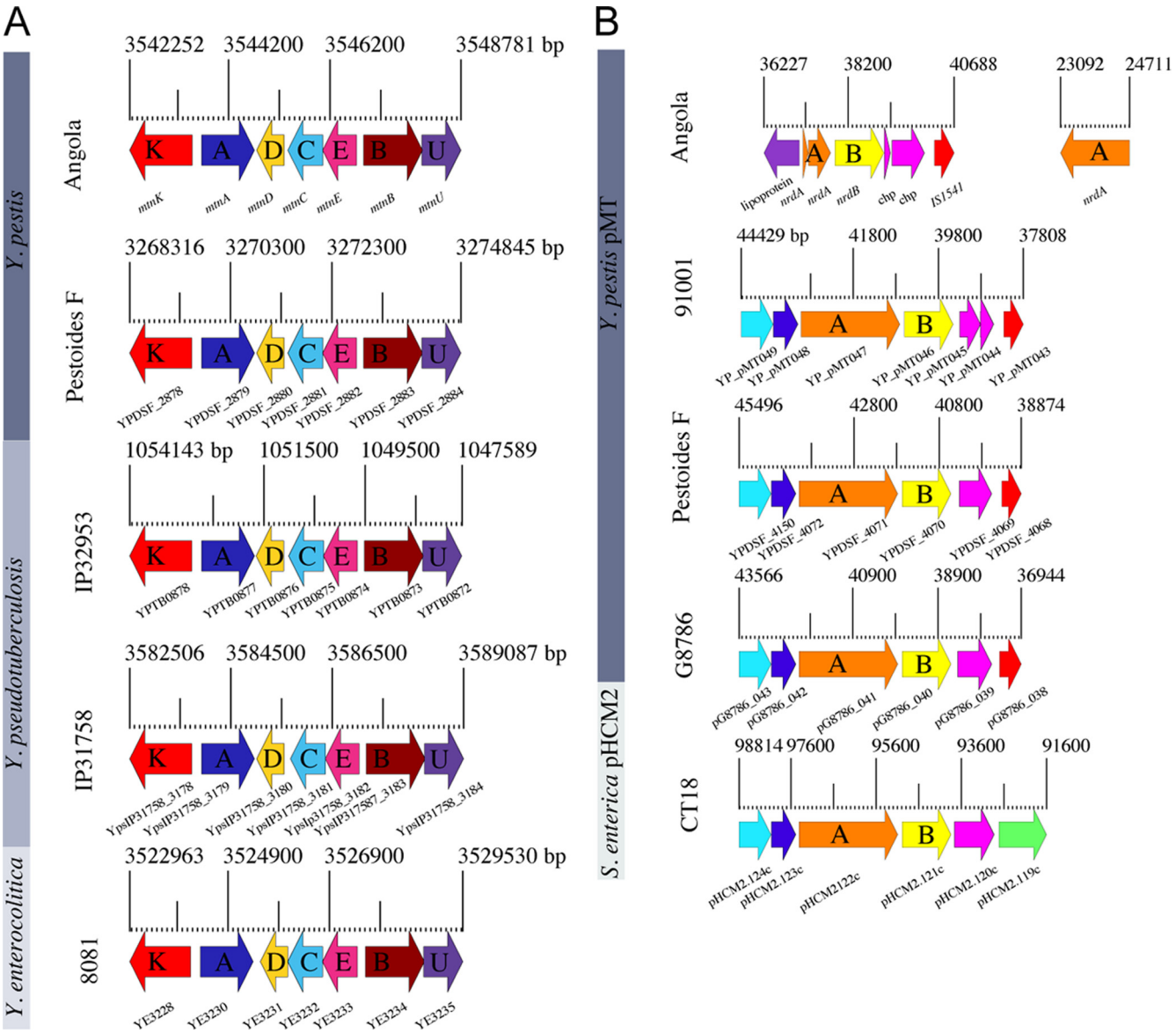

FIG. 2. Ancestral genome features of *Y. pestis* Angola. (A) Prevalence of the methionine salvage locus. Strain Angola and the deep-branching Pestoides group isolate F are the only known *Y. pestis* isolates that carry the methionine salvage pathway on their chromosomes. Its presence in the phylogenetic ancestors *Y. pseudotuberculosis* and *Y. enterocolitica* argues for a secondary loss of this metabolic property in descending *Y. pestis* isolates. The scale, in base pairs, indicates the genomic location of the methionine salvage locus composed of the seven genes *mtnKADCEBU*. Genes shared between these highly conserved and syntenically arranged loci are colored accordingly. (B) Prevalence of the *nrdAB* locus. Strain Angola encodes another locus on its chimeric plasmid, the ribonucleotide diphosphate reductase *nrdAB* operon, which most likely was lost secondarily in descending *Y. pestis* isolates. Corresponding loci are found only in other deep-branching *Y. pestis* strains: the Pestoides group isolates F and G8786 and the 0.PE4 microtus strain 91001. Besides *Y. pestis*, this locus also is present in the phylogenetically related pHCM2 plasmid of *S. enterica* CT18. In *Y. pestis* strain 91001, one of the two conserved hypothetical proteins appears to be degenerated (YP_pMT44, YP_pMT45). The scale, in base pairs, indicates the genomic location of the *nrdAB* operon. Genes shared between these loci are colored accordingly.

plasmid structure in this ancestral strain lets us speculate about a possible acquisition of both species-specific *Y. pestis* virulence plasmids in a single event during speciation from *Y. pseudotuberculosis*. The chimeric plasmid carries further ancestral signatures with homology to *Salmonella enterica* serovar Typhi CT18 plasmid pHCM2 (52), such as the ribonucleoside-diphosphate reductases *nrdAB* (Fig. 1B, 2B). This particular region, which is absent from all modern *Y. pestis* isolates, most likely was lost secondarily in the evolution of *Y. pestis*, as no difference in the overall G+C skew of this region and the plasmid backbone was observed (Fig. 1B). The observed prevalence of this fragment again supports a deeply rooted position of Angola in the *Y. pestis* phylogeny and also a close relationship to central Asian Pestoides isolates. The murine toxin component of the chimeric plasmid pMT-PCP carries a 6-kb region that displays more than 95% nucleotide similarity to the *Salmonella enterica* serovar Typhi CT18 plasmid pHCM2 (52) (Fig. 1B). In *Y. pestis* it is present only in three other deep-

branching isolates: the 0.PE4 microtus strain 91001 (59) and both substantially enlarged pMT plasmids of the Pestoides group, strains G8786 (137,036 bp) (28) and F (0.PE2a) (137,010 bp) (27). The prevalence strengthens the previously suggested phylogenetic relationship between the *Y. pestis* murine toxin plasmid and the *S. enterica* CT18 pHCM2 plasmid (55) and further supports the suggestion that they share ancestry as well as being able to exchange genetic material. The latter suggestion is supported by the high sequence similarity of the *Y. pestis* multidrug resistance (MDR)-conferring plasmid pIP1202 (26, 65) to IncA/C enteric MDR plasmids (52, 58, 65). This remnant 6-kb fragment encodes the alpha (*nrdA*) and beta (*nrdA*) subunits of the ribonucleoside-diphosphate reductase, which is involved in deoxyribonucleotide metabolism, and two hypothetical proteins with no assigned function (Fig. 2B). Comparative analyses of the plasmids *Y. pestis* pMT and *S. enterica* pHCM2 show that both the alpha subunit of the ribonucleoside phosphatase (33) and the conserved hypothetical proteins might be in the process of decay in strain Angola. Strain Angola carries two truncated *nrdA* pseudogenes (Fig. 2B, orange), while these genes appear to be intact and potentially functional in Pestoides group strains F and G8786 as well as in *S. enterica* CT18. Interestingly, in strain Angola, a second intact RNase copy is found 11.5 kb upstream from the first copy on the chimeric plasmid (Fig. 1B) and may functionally complement the degenerated *nrdA* pseudogenes.

Deletion of the plasmid-borne capsular antigen. Angola is the only *Y. pestis* isolate sequenced to date that lacks the complete pMT-borne capsular antigen (*caf*) on its chimeric plasmid (Fig. 1B). This species-specific operon forms the F1 capsular antigen and is syntenically organized in all previously studied isolates (13, 20, 28, 53, 59) (Fig. 3). The F1 locus is comprised of four genes that encode the structural subunit Caf1, the molecular chaperone Caf1M, the outer membrane anchor Caf1A, and the regulator Caf1R (40). The 5′-flanking region of the operon is highly conserved, but we found structural rearrangements in the adjacent 3′ region. It is not clear if the absence of the capsule in Angola is due to a secondary loss or represents an ancestral state. Indeed, the capsular antigen is not essential for the manifestation of *Y. pestis* virulence but rather contributes to pathogenicity (18). The ancestral position of Angola let us speculate in favor of a lateral acquisition of this virulence determinant during *Y. pestis* microevolution. This hypothesis is supported by a deviating G+C content within the antigen region observed for all analyzed F1-positive murine toxin plasmids. It is noteworthy that another pMT-borne virulence determinant, the murine toxin (*mtx*) (YpAngola_0119), also shows a G+C abnormality (Fig. 1B). Thus, it appears that both species-specific virulence determinants most likely were secondarily incorporated into the plasmid backbone, and their presence in *Y. pestis* does not represent the ancestral state of the pMT coding capacity (Fig. 1B). The genetic rearrangements at this locus might have been mechanistically facilitated by mobile genetic elements that are located downstream of the F1 locus. Although other nonencapsulated *Y. pestis* strains (54) as well as strains that express reduced amounts of the capsular antigen (68) have been reported from natural sources, their genomic architecture at this locus remains unknown. Such F1-negative strains are able to evade standard diagnostic assays specific for this surface-exposed antigen, and they potentially delay the essential immediate antibiotic treatment required to be administered according to the Centers for Disease Control and Prevention within the first 24 h postinfection. A possible emergence of this novel described Angola genotype raises questions about public health as well as future plague surveillance and treatment.

Assessment of virulence. The specific genetic make-up that allows *Y. pestis* to cause bubonic, pneumonic, and septicemic plague rather than enteric disease is not fully understood (73). The ancient nature of Angola makes it of particular importance in gaining insights into the evolution of *Y. pestis* virulence. Although the capsule could be an important virulence factor in certain rodent hosts in nature, strains lacking F1 retain virulence in laboratory animal models, including nonhuman primates (18, 70). The capsule is thought to be involved in *Y. pestis* pathogenesis, in particular by inhibiting phagocytosis, but is not a prerequisite for full virulence (25, 69). However, the capsule presumably is involved in the intimate bacterium-host interaction, and one can hypothesize that its absence in strain Angola, together with the other genetic polymorphisms identified in this isolate, affect the pathogenic potential. To test this hypothesis, we examined the virulence of Angola in three rodent plague models, the outbred mouse, inbred mouse, and guinea pig, testing different routes of infection.

The use of both mice and guinea pigs to assay virulence is based on the observation that nonepidemic, enzootic Pestoides subspecies show attenuated virulence phenotypes in guinea pigs, but typically they are fully virulent in the rodent superfamily Muroidea (7). Indeed, Angola did not cause lethality in the guinea pig after either 10^2- or 10^6-CFU subcutaneous doses, while the epidemic strain CO92 was 100% lethal at both doses (Table 2). A deficiency in the capsular antigen previously has been attributed to reduced virulence in guinea pigs (10). However, the lack of the capsular antigen in strain Angola does not necessarily indicate low virulence, but the first-ever reported complete absence of this surface-exposed capsule may affect the intimate bacterium-host interactions by altering the immune response of the mammalian host (15). A recent study of genetically engineered CAF-deficient mutants also suggests a role of the F1 antigen in promoting plague transmission by fleas (54). This finding also might hold true in the genetic background of strain Angola.

In Swiss Webster mice, Angola was fully virulent by the aerosol route but was significantly less virulent than a typical *Y. pestis* strain in a subcutaneous challenge. The 50% median lethal dose (LD_{50}) in aerosol-infected mice was 3.6×10^4 CFU, which is comparable to that of modern *Y. pestis* strains. However, the LD_{50} for Angola by the subcutaneous route was 1,153 CFU, which is relatively high compared to the LD_{50} of strain CO92 (2 CFU). Thus, there is a 500-fold difference in the LD_{50}s of these two strains by the parenteral route. The mean time to death (TTD) also was increased in Angola (8,000 CFU; 7.6 days), while for CO92 the TTD at a lower dose of 4,000 CFU was significantly less (4.8 days) (Table 2) (66).

Our data suggest that the Angola virulence in the subcutaneous mouse model, but not by the aerosol route of infection, is affected by the reported strain-specific polymorphisms that are intimately associated with its pathogenic potential (7, 10, 34). It is noteworthy that the ability of *Y. pestis* to cause a fatal pneumonic disease

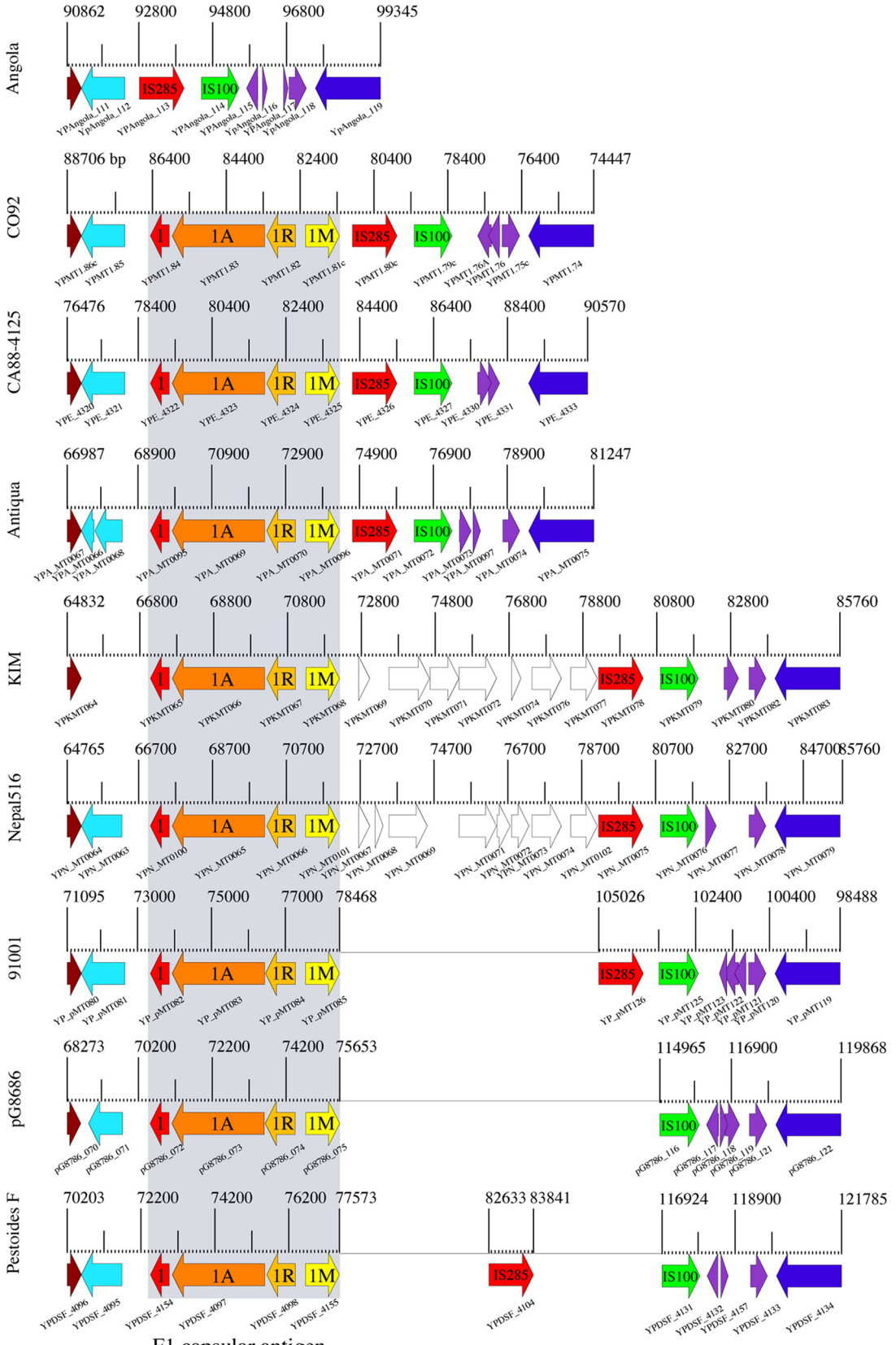

FIG. 3. Genomic architecture of the F1 capsular antigen. The F1 capsule is present and syntenically organized in all previously sequenced *Y. pestis* genomes, while strain Angola is the only currently known *Y. pestis* isolate that lacks the complete operon. Genes shared between these loci are colored accordingly.

TABLE 2. Virulence assay of *Y. pestis* Angola[a]

Assay and infection method	Inoculum (CFU)	TTD (days)	L/T
Swiss Webster mice LD_{50}			
Aerosol challenge	3.6×10^4	7.6 (8,000 CFU)	25/50
Subcutaneous challenge	1,153	7.6 (8,000 CFU)	25/50
Pathogenic potential in mice and guinea pigs (intradermal challenge)			
BALBc/inbred mice	10^2	8	6/18
	10^6	8.7	18/18
Hartley guinea pigs	10^2	NA	0/18
	10^6	NA	0/18

[a] The virulence of *Y. pestis* Angola was assayed in two laboratory rodent models following subcutaneous, intradermal, and aerosol challenge. Relative virulence was determined by lethality and mean time to death for each dose. L/T, observed lethality/total number of animals infected; TTD, mean time to death postexposure; NA, not applicable.

in mice appears to have evolved early, as it is present in this ancient strain. However, it appears to lack some of the capability of typical *Y. pestis* strains to invade via parenteral routes.

The identification of such a naturally occurring, albeit rare, F1-negative strain, along with its ability to cause lethal pneumonic plague, has major public health implications. The F1 antigen is an important genomic marker traditionally used in diagnostics. Its complete absence demonstrates that this locus is not an ideal candidate for the development of future plague vaccines, and other targets need to be identified (18, 25). It has been suggested that *Y. pestis* isolates such as Angola, which are virulent in mice but not in guinea pigs, present a reduced virulence in humans (7, 59). However, there are a number of documented problems with guinea pig plague models, and the projection of such animal model-based results on human plague virulence remains a point of debate (4).

Phylogenetic position of strain Angola. Detailed genome comparisons of this evolutionarily young pathogen enabled us to investigate important but rare genetic polymorphisms that determine the isolates' evolutionary relationships. The described genotypic signatures on the chromosome and plasmids of *Y. pestis* Angola clearly indicate a close relationship of strain Angola to the Pestoides group, which is suggestive for an ancestral phylogenetic positioning of Angola within the *Y. pestis* lineage (45) (Fig. 1, 2, and 4). The relationship of strain Angola to central Asian *Y. pestis* isolates is supported by our analysis of two previously deployed markers, such as the variable number of tandem repeats (VNTRs) and low-calcium-response V antigen (7, 45). We found that the pCD-borne *lcrV* gene of strain Angola (3) and the *Y. pestis* subsp. *hissarica* strain A-1728 (DQ489552) show an identical genetic make-up, carrying three nonsynonymous SNPs at positions 54, 215, and 817. This finding is consistent with their alleged ancestral status, as the African strain Angola and these analyzed Asian subspecies show a high degree of diversity in the *lcrV* antigen compared to those of descending modern *Y. pestis* isolates (see Table S2 in the supplemental material). However, due to the genetically homogenous nature of the *Y. pestis* population, the application of these genotyping methodologies is, in many cases, beyond the resolution threshold and cannot resolve the individual phylogenetic relationships of distinct *Y. pestis* isolates. To resolve the population structure, we applied an SNP-based genotyping methodology using the modern 1.ORI strain CO92 as the reference genome (8, 13, 20, 27, 53, 59, 63). In this study, we identified for the species a total of 424 synonymous SNPs (sSNPs) and 1,006 nonsynonymous SNPs (nsSNPs) (see Table S3 in the supplemental material), which is far more than previously reported (1). Genetic differences at the nucleotide level within the species previously have been attributed to less than 133 sSNPs and 349 nsSNPs (1, 2, 13). The Angola genome harbors the largest number of SNPs ever reported for a *Y. pestis* isolate compared to that of a modern 1.ORI isolate (i.e., *Y. pestis* CO92), carrying a total of 258 sSNPs and 502 nsSNPs. In addition, Angola features the largest number (210 sSNPs, 383 nsSNPs) of unique strain-specific sSNPs. Considering the large number of unique SNP identified in strain Angola, we investigated the possibility that this isolate is rapidly evolving through a mutator genotype. However, as evidenced in comparative nalidixic acid resistance assays (see Fig. S5 in the supplemental material), no significant differences were found in Angola mutability compared to that of CO92. In support of the nonmutator genotype, comprehensive analyses of genes encoding the DNA mismatch repair system MutHLS (YpAngola_A3242, YpAngola_A0701, and YpAngola_A3242) and nucleotide excision repair UvrABCD systems (YpAngola_A0751, YpAngola_A1430, YpAngola_A2053, and YpAngola_A0545) did not indicate any genetic differences that could affect Angola's mutation rate, as these loci are present and nondegenerated in strain Angola.

The SNP-based phylogeny (Fig. 4) reveals that Angola is one of the most ancestral and deep-rooted *Y. pestis* isolates analyzed to date, a finding consistent with the ancestral genome features we could identify in the Angola genome (Fig. 2 and 4; also see Fig. S4 in the supplemental material). Our phylogenetic analyses place strain Angola on the 0.PE3 branch and thus in a proximal position to the Pestoides group isolates F (0.PE2a) and 91001 (0.PE4) (1, 27). These two central Asian Pestoides group isolates are of different geographical origin than the African strain Angola, although the phylogenetic relationships of strains from central Asia and Africa have been observed previously by different classification methods, such as ribonucleoside or IS element genotyping (31, 49). The phylogeny further supports the hypothesis that biovars MED and ORI arose through parallel evolution from a biovar ANT progenitor due to the acquisition of independent mutations (29, 49). However, as demonstrated for strain Angola, grouping *Y. pestis* according to the classical definition of biovars on the basis of a few biochemical properties does not accurately reflect and resolve their phylogenetic relationship. This refined evolutionary history of *Y. pestis* clearly supports a grouping of *Y. pestis* into populations rather than biovars, as suggested by Achtman et al. (1).

The core genome and pangenome of the plague bacterium. We predicted, for the first time, the set of nonorthologous genes within the species, the *Y. pestis* pangenome, including chromosome- and plasmid-borne sequences of a given strain (47). This data set contained the genomes of four evolutionarily key strains isolated from the zoonotic rodent reservoir in foci of endemic plague in China (21a). The core genome and gene discovery computations are visualized in Fig. 5. Unlike the major role of lateral transfer that drives genome evolution

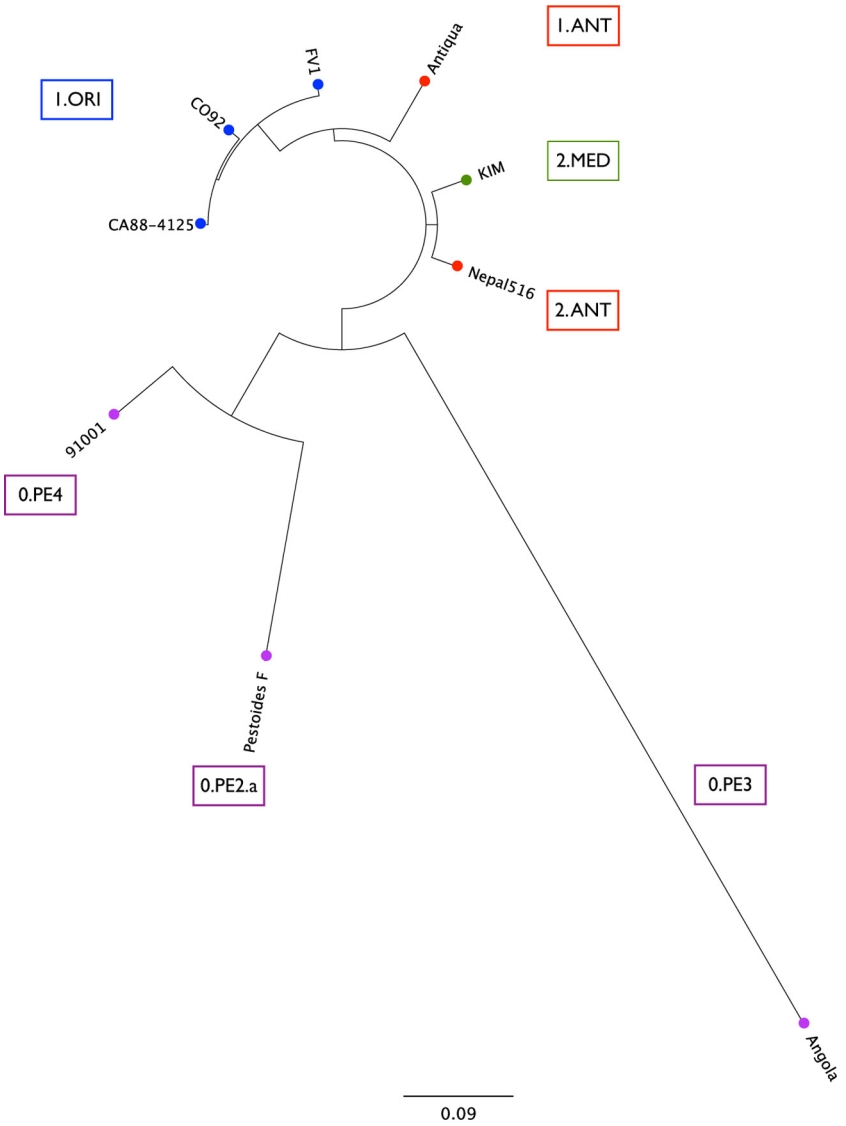

FIG. 4. Phylogenetic position of *Y. pestis* Angola. The phylogenetic tree is based on 424 sSNPs and 1,006 nsSNPs and reveals a deep branching of the 0.PE3 strain Angola within *Y. pestis*. Branch designations were assigned according to the nomenclature introduced by Achtman et al. (1). Strains biochemically classified into the same biovar are colored accordingly.

in the ancestor *Y. pseudotuberculosis* (22), the gene repertoire of *Y. pestis* is not significantly expanding by the acquisition of new genes (Fig. 5A). The core genome, i.e., genes present in all 14 genomes analyzed, consists of 3,668 protein-coding genes, of which more than 94% are present in *Y. pestis* CO92. The ancestral loci maintained in the Pestoides group isolates and Angola, such as the methionine salvage pathway, still are part of the global gene pool of *Y. pestis*, but they have undergone a reductive evolution in descending *Y. pestis* isolates (Fig. 2A; also see Fig. S4 in the supplemental material). On average, only 21 new genes would be discovered for each additional *Y. pestis* genome sequenced (Fig. 5B). These analyses clearly reflect the genetically homogenous nature of the *Y. pestis* population structure (see Table S1 in the supplemental material), and the results are comparable to data obtained for other evolutionarily young pathogens, such as *Bacillus anthracis* (47). The gene discovery rate was found to be significantly increased by the inclusion of *Y. pestis* strain IP275 (26) (Fig. 5B). This strain introduces more than 200 genes into the species gene pool, all of which are carried on the isolate-specific MDR plasmid pIP1202; none are found on its chromosome. This emphasizes the potential impact of such isolate-specific plasmid inventory in the genome evolution of *Y. pestis* (Fig. 5A) (1, 46). In this context, it is noteworthy that the closest relatives, *Y. pseudotuberculosis* and *Y. enterocolitica*, clearly have evolved by the acquisition of isolate-specific plasmids (22). The finding of the unique chimeric virulence plasmid, although it does not introduce novel genetic information into the species genome pool, provides further evidence for an open, yet-to-be-discovered *Y. pestis* panmobilome. Growing evidence suggests that the plasmid repertoire of *Y. pestis* is not restricted to the three classical virulence plasmids (24), and that its genetic inventory

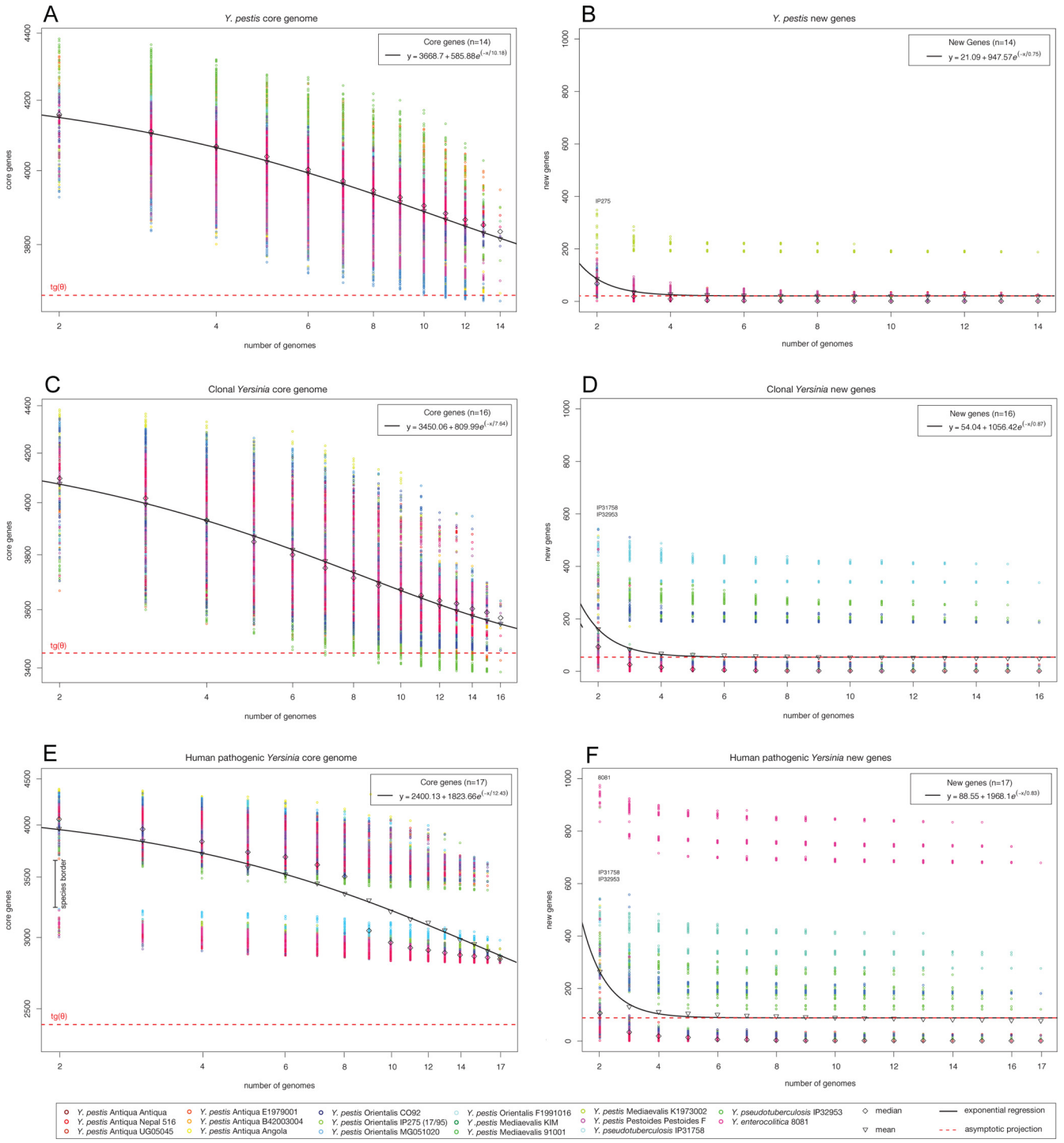

FIG. 5. Core genes and gene discovery in human pathogenic *Yersinia*. (A) Core genes. For each number of genomes n, circles are the permutations for *Y. pestis* values obtained for a sampling size of 1,000. Diamonds and triangles give median and mean values for each distribution. The curve represents the exponential regression of the least-squares fit of $F_{\text{core}}(n) = \kappa_c \exp[-n/\tau_c] + tg_c(\theta)$. The extrapolated core genome size is shown as a horizontal dashed red line. (B) Gene discovery. The numbers of new genes found are plotted for increasing values of n. The curve is the least-squares fit of the exponential decay $F_{\text{new}}(n) = \kappa_n \exp[-n/\tau_n] + tg_n(\theta)$ based on the means of the distribution. The value of $tg_n(\theta)$ shown represents the number of new genes asymptotically predicted for further genome sequencing. Core genes (C, E) and gene discovery (D, F) when *Y. pseudotuberculosis* strains IP31758 and IP32953 and *Y. enterocolitica* 8081 are included.

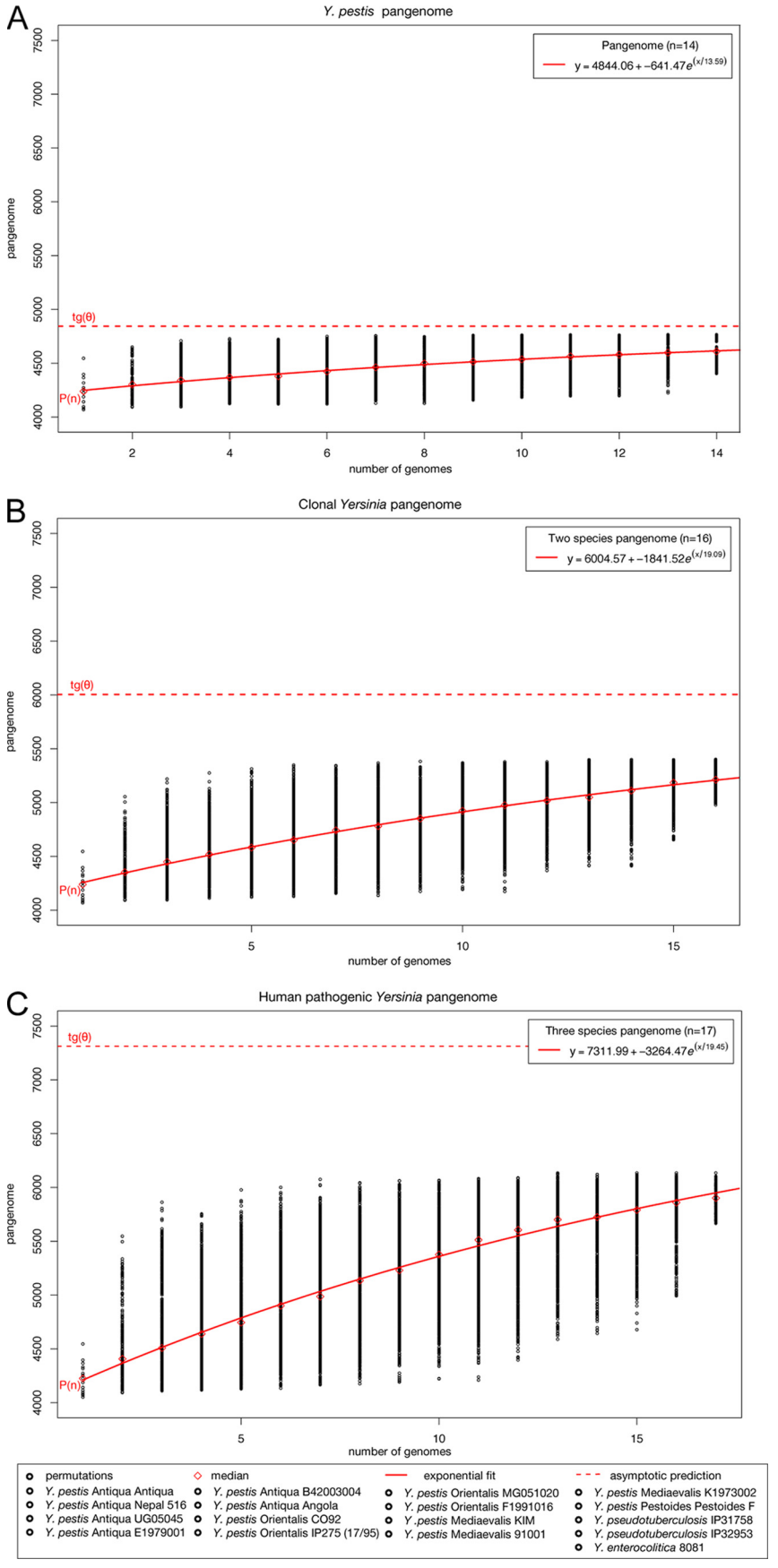
A
Y. pestis pangenome
Pangenome (n=14)
y = 4844.06 + −641.47e^(x/13.59)
pangenome
tg(θ)
P(n)
number of genomes
B
Clonal Yersinia pangenome
Two species pangenome (n=16)
y = 6004.57 + −1841.52e^(x/19.09)
pangenome
tg(θ)
P(n)
number of genomes
C
Human pathogenic Yersinia pangenome
Three species pangenome (n=17)
y = 7311.99 + −3264.47e^(x/19.45)
pangenome
tg(θ)
P(n)
number of genomes
permutations
median
exponential fit
asymptotic prediction
Y. pestis Antiqua Antiqua
Y. pestis Antiqua Nepal 516
Y. pestis Antiqua UG05045
Y. pestis Antiqua E1979001
Y. pestis Antiqua B42003004
Y. pestis Antiqua Angola
Y. pestis Orientalis CO92
Y. pestis Orientalis IP275 (17/95)
Y. pestis Orientalis MG051020
Y. pestis Orientalis F1991016
Y .pestis Mediaevalis KIM
Y. pestis Mediaevalis 91001
Y. pestis Mediaevalis K1973002
Y. pestis Pestoides Pestoides F
Y. pseudotuberculosis IP31758
Y. pseudotuberculosis IP32953
Y. enterocolitica 8081

is partly shared, either due to common ancestry or lateral exchange, with other human and zoonotic bacterial pathogens, such as *S. enterica*, *S. enterica* serovar Typhimurium (52, 65), *Klebsiella pneumoniae* (58), and *Streptococcus equi* (36). The potential dissemination of genetic information between *Y. pestis* and other pathogens might be advantageous for strain-specific niche adaptations and bacterial fitness but also potentially impacts the pathogenic potential and should be considered in the future program development for plague surveillance, prophylaxis, and treatment.

Crossing the species border, we included the two other human pathogenic *Yersinia* species: *Y. pseudotuberculosis*, represented by the far-eastern scarlatiniform and pseudotuberculosis-causing strains IP31758 and IP32953 (12, 22), and *Y. enterocolitica* 8081 (61). When *Y. pseudotuberculosis* is included, the number of conserved core genes within these two species decreases slightly to 3,450 genes, while the predicted number of new genes for each new genome sequenced increases to 54 (Fig. 5E and F). Given the high degree of proteome conservation between *Y. pestis* and its progenitor *Y. pseudotuberculosis* (see Table S1 in the supplemental material), the species border is not well defined and the computed core gene sets differ by only 218 genes. This finding is supported by the close phylogenetic relationship between these two *Yersinia* species (12, 22) (Fig. 1A). In contrast, the evolutionary distance between *Y. pseudotuberculosis* and *Y. pestis* to the phylogenetically distant *Y. enterocolitica* strain 8081 is clearly visible in Fig. 5E and F. The conserved gene set shrinks by 30% to 2,400 genes present in all three human pathogenic *Yersinia* species sequenced to date. This decrease reflects the estimated 1.9 million years of evolution separating *Y. pseudotuberculosis* and its phylogenetic descendants *Y. pestis* and *Y. enterocolitica* (2).

The predicted pangenome defines the global gene reservoir, the total number of genes found at least once among the 14 genomes analyzed, of this group and is estimated to consist of 4,844 genes for *Y. pestis* (Fig. 6A), and it is only 19% larger than the proteome of *Y. pestis* strain CO92 (53). Our pangenome computation indicates that the *Y. pestis* core genome reaches a minimum of genes and remains relatively constant, even as more genomes are added, indicating that *Y. pestis* as a species has a closed pangenome. On the contrary, in a species featuring an open pangenome, such as *Escherichia coli*, the predicted pangenome size was found to be almost 75% larger than the average genome size of the species (64). The global *Yersinia* pangenomes are predicted to consist of a gene pool of 6,004 genes for *Y. pestis* and *Y. pseudotuberculosis* (Fig. 6B) and 7,311 genes when *Y. enterocolitica* is included in the analysis (Fig. 6C). The 25 and 50% increases in pangenome sizes compared to that of the *Y. pestis*-only pangenome mirrors the phylogenetic relationships and individual traits of genome evolution within this group of organisms. The differences in the global gene pool across the species borders is caused by the observed reductive evolution in *Y. pestis* (22) (Fig. 2 and 4; also see Fig. S4 in the supplemental material) and by the influx of genetic material, such as the horizontal acquisition of species- and isolate-specific plasmids, together with the incorporation of different genetic information into the chromosome of these two enteric *Yersinia* species (22, 61).

DISCUSSION

Evolutionary considerations. The sequencing and phylogenomic analyses of this evolutionary *Y. pestis* key isolate advances our understanding of the speciation of this highly host-adapted pathogen from its enteric progenitor, *Y. pseudotuberculosis*. This study identified distinct adaptive microevolutionary traits that shaped the genome organization and gene inventory of this atypical African isolate and let us conclude that Angola belongs to one of the most ancient *Y. pestis* lineages thus far sequenced. Atypical *Y. pestis* strains have been reported to exist in natural foci in central Asia and are classified as the Pestoides group of isolates to acknowledge their distinct genetic, biochemical, and virulence properties (7, 70). However, strain Angola is the first African *Y. pestis* isolate that can be identified as a representative of these ancestral lineages. Making use of the newly identified Angola genotypic and phenotypic characteristics will help to achieve a higher phylogenetic resolution in this genetically homogenous pathogen. The microevolution seems to be driven by isolate-specific genetic polymorphisms and by a high rate of intrachromosomal rearrangements driven by IS elements. Because the Angola genome has experienced such expansion, it is suggested that this phenomenon occurred soon after the split of *Y. pestis* from *Y. pseudotuberculosis*. Its mobilome further demonstrates that the *Y. pestis* plasmid repertoire is not restricted to the classical virulence plasmids. The unique chimeric virulence plasmid clearly shows the major impact of an isolate-specific plasmid inventory in the genome evolution in this otherwise genetically homogenous pathogen and provides further evidence for an open panmobilome.

Genomic plasticity in *Y. pestis*. The unique genetic traits in the Angola genome identified in this study, together with the largest number of isolate-specific SNPs, clearly support the existence of a yet-undiscovered genetic diversity within *Y. pestis* that is not as limited as previously thought. Thus, to gain further insights into the existing and evolving genetic diversity of *Y. pestis*, it is essential to continue gathering additional sequence data. The possible emergence of fully virulent F1-negative isolates capable of evading standard diagnostic assays raises major public health concerns and should be considered in future plague surveillance. Owing to the critical importance of *Y. pestis* for human health, the key to understanding the emergence and impact of such previously unknown genotypes,

FIG. 6. Pangenome of human pathogenic *Yersinia*. (A) Pangenome of *Y. pestis*. The total number of genes found according to the pangenome analyses is shown for increasing values of the number *n* of *Yersinia* genomes sequenced using medians and an exponential fit. Red diamonds indicate the means of the distributions. The dashed line represents the total number of genes that comprise the respective pangenome asymptotically predicted for further genome sequencing. (B) The two-species pangenome computed for *Y. pestis* and the closest evolutionary ancestor *Y. pseudotuberculosis*. (C) The three-species *Yersinia* pangenome computed for *Y. pestis*, *Y. pseudotuberculosis*, and *Y. enterocolitica*.

some of which are associated with plague pathogenicity and epidemiology, resides in the sampling and characterization of more isolates.

ACKNOWLEDGMENTS

This work was supported with federal funds from the National Institute of Allergy and Infectious Diseases, National Institutes of Health, Department of Health and Human Services, under NIAID contract N01 AI-30071, and Defense Threat Reduction Agency JSTO-CBD project 1.1A0021_07_RD_B (P.W.L.).

Opinions, interpretations, conclusions, and recommendations are those of the authors and are not necessarily endorsed by the U.S. Army.

We thank Richard Borschel for performing the guinea pig assay.

Research was conducted in compliance with the Animal Welfare Act and other federal statutes and regulations involving animals and adheres to the principles stated in the Guide for the Care and Use of Laboratory Animals, National Research Council, 1996. The facility where this animal research was conducted is fully accredited by the Association for Assessment and Accreditation of Laboratory Animal Care International.

REFERENCES

1. **Achtman, M., G. Morelli, P. Zhu, T. Wirth, I. Diehl, B. Kusecek, A. J. Vogler, D. M. Wagner, C. J. Allender, W. R. Easterday, V. Chenal-Francisque, P. Worsham, N. R. Thomson, J. Parkhill, L. E. Lindler, E. Carniel, and P. Keim.** 2004. Microevolution and history of the plague bacillus, Yersinia pestis. Proc. Natl. Acad. Sci. USA **101:**17837–17842.
2. **Achtman, M., K. Zurth, G. Morelli, G. Torrea, A. Guiyoule, and E. Carniel.** 1999. Yersinia pestis, the cause of plague, is a recently emerged clone of Yersinia pseudotuberculosis. Proc. Natl. Acad. Sci. USA **96:**14043–14048.
3. **Adair, D. M., P. L. Worsham, K. K. Hill, A. M. Klevytska, P. J. Jackson, A. M. Friedlander, and P. Keim.** 2000. Diversity in a variable-number tandem repeat from Yersinia pestis. J. Clin. Microbiol. **38:**1516–1519.
4. **Adamovicz, J. L., and P. L. Worsham.** 2006. Plague, p. 107–135. *In* J. R. Swearengen (ed.), Biodefense: research methodology and animal models. CRC Press Taylor & Francis Group, Boca Raton, FL.
5. **Altschul, S. F., T. L. Madden, A. A. Schaffer, J. Zhang, Z. Zhang, W. Miller, and D. J. Lipman.** 1997. Gapped BLAST and PSI-BLAST: a new generation of protein database search programs. Nucleic Acids Res. **25:**3389–3402.
6. **Anderson, G. W., Jr., S. E. Leary, E. D. Williamson, R. W. Titball, S. L. Welkos, P. L. Worsham, and A. M. Friedlander.** 1996. Recombinant V antigen protects mice against pneumonic and bubonic plague caused by F1-capsule-positive and -negative strains of Yersinia pestis. Infect. Immun. **64:**4580–4585.
7. **Anisimov, A. P., L. E. Lindler, and G. B. Pier.** 2004. Intraspecific diversity of Yersinia pestis. Clin. Microbiol. Rev. **17:**434–464.
8. **Auerbach, R. K., A. Tuanyok, W. S. Probert, L. Kenefic, A. J. Vogler, D. C. Bruce, C. Munk, T. S. Brettin, M. Eppinger, J. Ravel, D. M. Wagner, and P. Keim.** 2007. Yersinia pestis evolution on a small timescale: comparison of whole genome sequences from North America. PLoS One **2:**e770.
9. **Bearden, S. W., C. Sexton, J. Pare, J. M. Fowler, C. G. Arvidson, L. Yerman, R. E. Viola, and R. R. Brubaker.** 2009. Attenuated enzootic (pestoides) isolates of Yersinia pestis express active aspartase. Microbiology **155:**198–209.
10. **Burrows, T. W.** 1957. Virulence of Pasteurella pestis. Nature **179:**1246–1247.
11. **Carniel, E., and B. J. Hinnebusch (ed.).** 2004. Yersinia molecular and cellular biology. Horizon Biosciences, Norfolk NR18 0JA, United Kingdom.
12. **Chain, P. S., E. Carniel, F. W. Larimer, J. Lamerdin, P. O. Stoutland, W. M. Regala, A. M. Georgescu, L. M. Vergez, M. L. Land, V. L. Motin, R. R. Brubaker, J. Fowler, J. Hinnebusch, M. Marceau, C. Medigue, M. Simonet, V. Chenal-Francisque, B. Souza, D. Dacheux, J. M. Elliott, A. Derbise, L. J. Hauser, and E. Garcia.** 2004. Insights into the evolution of Yersinia pestis through whole-genome comparison with Yersinia pseudotuberculosis. Proc. Natl. Acad. Sci. USA **101:**13826–13831.
13. **Chain, P. S. G., P. Hu, S. A. Malfatti, L. Radnedge, F. Larimer, L. M. Vergez, P. Worsham, M. C. Chu, and G. L. Andersen.** 2006. Complete genome sequence of Yersinia pestis strains Antiqua and Nepal516: evidence of gene reduction in an emerging pathogen. J. Bacteriol. **188:**4453–4463.
14. **Chu, M. C., X. Q. Dong, X. Zhou, and C. F. Garon.** 1998. A cryptic 19-kilobase plasmid associated with U.S. isolates of Yersinia pestis: a dimer of the 9.5-kilobase plasmid. Am. J. Trop. Med. Hyg. **59:**679–686.
15. **Cornelius, C. A., L. E. Quenee, D. Elli, N. A. Ciletti, and O. Schneewind.** 2009. Yersinia pestis IS1541 transposition provides for escape from plague immunity. Infect. Immun. **77:**1807–1816.
16. **Cummings, C. A., M. M. Brinig, P. W. Lepp, S. van de Pas, and D. A. Relman.** 2004. Bordetella species are distinguished by patterns of substantial gene loss and host adaptation. J. Bacteriol. **186:**1484–1492.
17. **Darling, A. E., I. Miklos, and M. A. Ragan.** 2008. Dynamics of genome rearrangement in bacterial populations. PLoS Genet. **4:**e1000128.
18. **Davis, K. J., D. L. Fritz, M. L. Pitt, S. L. Welkos, P. L. Worsham, and A. M. Friedlander.** 1996. Pathology of experimental pneumonic plague produced by fraction 1-positive and fraction 1-negative Yersinia pestis in African green monkeys (Cercopithecus aethiops). Arch. Pathol. Lab. Med. **120:**156–163.
19. **Delcher, A. L., A. Phillippy, J. Carlton, and S. L. Salzberg.** 2002. Fast algorithms for large-scale genome alignment and comparison. Nucleic Acids Res. **30:**2478–2483.
20. **Deng, W., V. Burland, G. Plunkett, 3rd, A. Boutin, G. F. Mayhew, P. Liss, N. T. Perna, D. J. Rose, B. Mau, S. Zhou, D. C. Schwartz, J. D. Fetherston, L. E. Lindler, R. R. Brubaker, G. V. Plano, S. C. Straley, K. A. McDonough, M. L. Nilles, J. S. Matson, F. R. Blattner, and R. D. Perry.** 2002. Genome sequence of Yersinia pestis KIM. J. Bacteriol. **184:**4601–4611.
21. **Devignat, R.** 1953. Geographical distribution of three species of Pasteurella pestis. Schweiz. Z Pathol. Bakteriol. **16:**509–514.

21a. **Eppinger, M., Z. Guo, Y. Sebastian, Y. Song, L. E. Lindler, R. Yang, and J. Ravel.** 2009. Draft genome sequences of *Yersinia pestis* isolates from natural foci of endemic plague in China. J. Bacteriol. **191:**7628–7629.

22. **Eppinger, M., M. J. Rosovitz, W. F. Fricke, D. A. Rasko, G. Kokorina, C. Fayolle, L. E. Lindler, E. Carniel, and J. Ravel.** 2007. The complete genome sequence of Yersinia pseudotuberculosis IP31758, the causative agent of Far East scarlet-like fever. PLoS Genet. **3:**e142.
23. **Ewing, B., L. Hillier, M. C. Wendl, and P. Green.** 1998. Base-calling of automated sequencer traces using phred. I. Accuracy assessment. Genome Res. **8:**175–185.
24. **Filippov, A. A., N. S. Solodovnikov, L. M. Kookleva, and O. A. Protsenko.** 1990. Plasmid content in Yersinia pestis strains of different origin. FEMS Microbiol. Lett. **55:**45–48.
25. **Friedlander, A. M., S. L. Welkos, P. L. Worsham, G. P. Andrews, D. G. Heath, G. W. Anderson, Jr., M. L. Pitt, J. Estep, and K. Davis.** 1995. Relationship between virulence and immunity as revealed in recent studies of the F1 capsule of Yersinia pestis. Clin. Infect. Dis. **21**(Suppl. 2)**:**S178–S181.
26. **Galimand, M., A. Guiyoule, G. Gerbaud, B. Rasoamanana, S. Chanteau, E. Carniel, and P. Courvalin.** 1997. Multidrug resistance in Yersinia pestis mediated by a transferable plasmid. N. Engl. J. Med. **337:**677–680.
27. **Garcia, E., P. Worsham, S. Bearden, S. Malfatti, D. Lang, F. Larimer, L. Lindler, and P. Chain.** 2007. Pestoides F, an atypical Yersinia pestis strain from the former Soviet Union. Adv. Exp. Med. Biol. **603:**17–22.
28. **Golubov, A., H. Neubauer, C. Nolting, J. Heesemann, and A. Rakin.** 2004. Structural organization of the pFra virulence-associated plasmid of rhamnose-positive Yersinia pestis. Infect. Immun. **72:**5613–5621.
29. **Gonzalez, M. D., C. A. Lichtensteiger, R. Caughlan, and E. R. Vimr.** 2002. Conserved filamentous prophage in Escherichia coli O18:K1:H7 and Yersinia pestis biovar orientalis. J. Bacteriol. **184:**6050–6055.
30. **Guindon, S., F. Lethiec, P. Duroux, and O. Gascuel.** 2005. PHYML Online—a web server for fast maximum likelihood-based phylogenetic inference. Nucleic Acids Res. **33:**W557–W559.
31. **Guiyoule, A., F. Grimont, I. Iteman, P. A. Grimont, M. Lefevre, and E. Carniel.** 1994. Plague pandemics investigated by ribotyping of Yersinia pestis strains. J. Clin. Microbiol. **32:**634–641.
32. **Guyton, A. C.** 1947. Measurement of the respiratory volumes of laboratory animals. Am. J. Physiol. **150:**70.
33. **Hacker, J., B. Hochhut, B. Middendorf, G. Schneider, C. Buchrieser, G. Gottschalk, and U. Dobrindt.** 2004. Pathogenomics of mobile genetic elements of toxigenic bacteria. Int. J. Med. Microbiol. **293:**453–461.
34. **Haiko, J., M. Kukkonen, J. J. Ravantti, B. Westerlund-Wikstrom, and T. K. Korhonen.** 2009. The single substitution I259T conserved in the plasminogen activator Pla of pandemic Yersinia pestis branches enhances fibrinolytic activity. J. Bacteriol. **191:**4758–4766.
35. **Hasegawa, M., H. Kishino, and T. Yano.** 1985. Dating of the human-ape splitting by a molecular clock of mitochondrial DNA. J. Mol. Evol. **22:**160–174.
36. **Holden, M. T., Z. Heather, R. Paillot, K. F. Steward, K. Webb, F. Ainslie, T. Jourdan, N. C. Bason, N. E. Holroyd, K. Mungall, M. A. Quail, M. Sanders, M. Simmonds, D. Willey, K. Brooks, D. M. Aanensen, B. G. Spratt, K. A. Jolley, M. C. Maiden, M. Kehoe, N. Chanter, S. D. Bentley, C. Robinson, D. J. Maskell, J. Parkhill, and A. S. Waller.** 2009. Genomic evidence for the evolution of Streptococcus equi: host restriction, increased virulence, and genetic exchange with human pathogens. PLoS Pathog. **5:**e1000346.
37. **Huson, D. H., and D. Bryant.** 2006. Application of phylogenetic networks in evolutionary studies. Mol. Biol. Evol. **23:**254–267.
38. **Huson, D. H., K. Reinert, S. A. Kravitz, K. A. Remington, A. L. Delcher, I. M. Dew, M. Flanigan, A. L. Halpern, Z. Lai, C. M. Mobarry, G. G. Sutton, and E. W. Myers.** 2001. Design of a compartmentalized shotgun assembler for the human genome. Bioinformatics **17**(Suppl. 1)**:**S132–S139.
39. **Jaccard, P.** 1908. Nouvelles recherches sur la distribution florale. Bull. Soc. Vaudoise Sci. Nat. **44:**223–270.
40. **Knight, S. D.** 2007. Structure and assembly of Yersinia pestis F1 antigen. Adv. Exp. Med. Biol. **603:**74–87.
41. **Kukleva, L. M., G. A. Eroshenko, V. E. Kuklev, N. Shavina, M. Krasnov Ia,**

N. P. Guseva, and V. V. Kutyrev. 2008. A study of the nucleotide sequence variability of rha locus genes of Yersinia pestis main and non-main subspecies. Mol. Gen. Mikrobiol. Virusol. **2008:**23–27.
42. **Kurtz, S., A. Phillippy, A. L. Delcher, M. Smoot, M. Shumway, C. Antonescu, and S. L. Salzberg.** 2004. Versatile and open software for comparing large genomes. Genome Biol. **5:**R12.
43. **Lathem, W. W., P. A. Price, V. L. Miller, and W. E. Goldman.** 2007. A plasminogen-activating protease specifically controls the development of primary pneumonic plague. Science **315:**509–513.
44. **Leal-Balbino, T. C., N. C. Leal, C. V. Lopes, and A. M. Almeida.** 2004. Differences in the stability of the plasmids of Yersinia pestis cultures in vitro: impact on virulence. Mem. Inst. Oswaldo Cruz **99:**727–732.
45. **Li, Y., Y. Cui, Y. Hauck, M. E. Platonov, E. Dai, Y. Song, Z. Guo, C. Pourcel, S. V. Dentovskaya, A. P. Anisimov, R. Yang, and G. Vergnaud.** 2009. Genotyping and phylogenetic analysis of Yersinia pestis by MLVA: insights into the worldwide expansion of Central Asia plague foci. PLoS One **4:**e6000.
46. **Li, Y., E. Dai, Y. Cui, M. Li, Y. Zhang, M. Wu, D. Zhou, Z. Guo, X. Dai, B. Cui, Z. Qi, Z. Wang, H. Wang, X. Dong, Z. Song, J. Zhai, Y. Song, and R. Yang.** 2008. Different region analysis for genotyping Yersinia pestis isolates from China. PLoS One **3:**e2166.
47. **Medini, D., C. Donati, H. Tettelin, V. Masignani, and R. Rappuoli.** 2005. The microbial pan-genome. Curr. Opin. Genet. Dev. **15:**589–594.
48. **Mollaret, H. H., and C. Mollaret.** 1965. Melibiose fermentation in the genus Yersina and its importance in the diagnosis of the varieties of Y. pestis. Bull. Soc. Pathol. Exot. Filiales **58:**154–156.
49. **Motin, V. L., A. M. Georgescu, J. M. Elliott, P. Hu, P. L. Worsham, L. L. Ott, T. R. Slezak, B. A. Sokhansanj, W. M. Regala, R. R. Brubaker, and E. Garcia.** 2002. Genetic variability of Yersinia pestis isolates as predicted by PCR-based IS100 genotyping and analysis of structural genes encoding glycerol-3-phosphate dehydrogenase (glpD). J. Bacteriol. **184:**1019–1027.
50. **Nagamatsu, T., H. Yamasaki, T. Hirota, M. Yamato, Y. Kido, M. Shibata, and F. Yoneda.** 1993. Syntheses of 3-substituted 1-methyl-6-phenylpyrimido[5,4-e]-1,2,4-triazine-5,7(1H,6H)-diones (6-phenyl analogs of toxoflavin) and their 4-oxides, and evaluation of antimicrobial activity of toxoflavins and their analogs. Chem. Pharm. Bull. (Tokyo) **41:**362–368.
51. **Nelson, K. E., R. A. Clayton, S. R. Gill, M. L. Gwinn, R. J. Dodson, D. H. Haft, E. K. Hickey, J. D. Peterson, W. C. Nelson, K. A. Ketchum, L. McDonald, T. R. Utterback, J. A. Malek, K. D. Linher, M. M. Garrett, A. M. Stewart, M. D. Cotton, M. S. Pratt, C. A. Phillips, D. Richardson, J. Heidelberg, G. G. Sutton, R. D. Fleischmann, J. A. Eisen, O. White, S. L. Salzberg, H. O. Smith, J. C. Venter, and C. M. Fraser.** 1999. Evidence for lateral gene transfer between Archaea and bacteria from genome sequence of Thermotoga maritima. Nature **399:**323–329.
52. **Parkhill, J., G. Dougan, K. D. James, N. R. Thomson, D. Pickard, J. Wain, C. Churcher, K. L. Mungall, S. D. Bentley, M. T. Holden, M. Sebaihia, S. Baker, D. Basham, K. Brooks, T. Chillingworth, P. Connerton, A. Cronin, P. Davis, R. M. Davies, L. Dowd, N. White, J. Farrar, T. Feltwell, N. Hamlin, A. Haque, T. T. Hien, S. Holroyd, K. Jagels, A. Krogh, T. S. Larsen, S. Leather, S. Moule, P. O'Gaora, C. Parry, M. Quail, K. Rutherford, M. Simmonds, J. Skelton, K. Stevens, S. Whitehead, and B. G. Barrell.** 2001. Complete genome sequence of a multiple drug resistant Salmonella enterica serovar Typhi CT18. Nature **413:**848–852.
53. **Parkhill, J., B. W. Wren, N. R. Thomson, R. W. Titball, M. T. Holden, M. B. Prentice, M. Sebaihia, K. D. James, C. Churcher, K. L. Mungall, S. Baker, D. Basham, S. D. Bentley, K. Brooks, A. M. Cerdeno-Tarraga, T. Chillingworth, A. Cronin, R. M. Davies, P. Davis, G. Dougan, T. Feltwell, N. Hamlin, S. Holroyd, K. Jagels, A. V. Karlyshev, S. Leather, S. Moule, P. C. Oyston, M. Quail, K. Rutherford, M. Simmonds, J. Skelton, K. Stevens, S. Whitehead, and B. G. Barrell.** 2001. Genome sequence of Yersinia pestis, the causative agent of plague. Nature **413:**523–527.
54. **Phillips, A. P., B. C. Morris, D. Hall, M. Glenister, and J. E. Williams.** 1988. Identification of encapsulated and non-encapsulated Yersinia pestis by immunofluorescence tests using polyclonal and monoclonal antibodies. Epidemiol. Infect. **101:**59–73.
55. **Prentice, M. B., K. D. James, J. Parkhill, S. G. Baker, K. Stevens, M. N. Simmonds, K. L. Mungall, C. Churcher, P. C. Oyston, R. W. Titball, B. W. Wren, J. Wain, D. Pickard, T. T. Hien, J. J. Farrar, and G. Dougan.** 2001. Yersinia pestis pFra shows biovar-specific differences and recent common ancestry with a Salmonella enterica serovar Typhi plasmid. J. Bacteriol. **183:**2586–2594.
56. **Rasko, D. A., G. S. Myers, and J. Ravel.** 2005. Visualization of comparative genomic analyses by BLAST score ratio. BMC Bioinformatics **6:**2.
57. **Sekowska, A., V. Denervaud, H. Ashida, K. Michoud, D. Haas, A. Yokota, and A. Danchin.** 2004. Bacterial variations on the methionine salvage pathway. BMC Microbiol. **4:**9.
58. **Soler Bistué, A. J., D. Birshan, A. P. Tomaras, M. Dandekar, T. Tran, J. Newmark, D. Bui, N. Gupta, K. Hernandez, R. Sarno, A. Zorreguieta, L. A. Actis, and M. E. Tolmasky.** 2008. Klebsiella pneumoniae multiresistance plasmid pMET1: similarity with the Yersinia pestis plasmid pCRY and integrative conjugative elements. PLoS One **3:**e1800.
59. **Song, Y., Z. Tong, J. Wang, L. Wang, Z. Guo, Y. Han, J. Zhang, D. Pei, D. Zhou, H. Qin, X. Pang, Y. Han, J. Zhai, M. Li, B. Cui, Z. Qi, L. Jin, R. Dai, F. Chen, S. Li, C. Ye, Z. Du, W. Lin, J. Wang, J. Yu, H. Yang, J. Wang, P. Huang, and R. Yang.** 2004. Complete genome sequence of Yersinia pestis strain 91001, an isolate avirulent to humans. DNA Res. **11:**179–197.
60. **Summers, D. K., C. W. Beton, and H. L. Withers.** 1993. Multicopy plasmid instability: the dimer catastrophe hypothesis. Mol. Microbiol. **8:**1031–1038.
61. **Thomson, N. R., S. Howard, B. W. Wren, M. T. Holden, L. Crossman, G. L. Challis, C. Churcher, K. Mungall, K. Brooks, T. Chillingworth, T. Feltwell, Z. Abdellah, H. Hauser, K. Jagels, M. Maddison, S. Moule, M. Sanders, S. Whitehead, M. A. Quail, G. Dougan, J. Parkhill, and M. B. Prentice.** 2006. The complete genome sequence and comparative genome analysis of the high pathogenicity Yersinia enterocolitica strain 8081. PLoS Genet **2:**e206.
62. **Torrea, G., V. Chenal-Francisque, A. Leclercq, and E. Carniel.** 2006. Efficient tracing of global isolates of *Yersinia pestis* by restriction fragment length polymorphism analysis using three insertion sequences as probes. J. Clin. Microbiol. **44:**2084–2092.
63. **Touchman, J. W., D. M. Wagner, J. Hao, S. D. Mastrian, M. K. Shah, A. J. Vogler, C. J. Allender, E. A. Clark, D. S. Benitez, D. J. Youngkin, J. M. Girard, R. K. Auerbach, S. M. Beckstrom-Sternberg, and P. Keim.** 2007. A North American Yersinia pestis draft genome sequence: SNPs and phylogenetic analysis. PLoS One **2:**e220.
64. **Touchon, M., C. Hoede, O. Tenaillon, V. Barbe, S. Baeriswyl, P. Bidet, E. Bingen, S. Bonacorsi, C. Bouchier, O. Bouvet, A. Calteau, H. Chiapello, O. Clermont, S. Cruveiller, A. Danchin, M. Diard, C. Dossat, M. E. Karoui, E. Frapy, L. Garry, J. M. Ghigo, A. M. Gilles, J. Johnson, C. Le Bouguenec, M. Lescat, S. Mangenot, V. Martinez-Jehanne, I. Matic, X. Nassif, S. Oztas, M. A. Petit, C. Pichon, Z. Rouy, C. S. Ruf, D. Schneider, J. Tourret, B. Vacherie, D. Vallenet, C. Medigue, E. P. Rocha, and E. Denamur.** 2009. Organised genome dynamics in the Escherichia coli species results in highly diverse adaptive paths. PLoS Genet. **5:**e1000344.
65. **Welch, T. J., W. F. Fricke, P. F. McDermott, D. G. White, M. L. Rosso, D. A. Rasko, M. K. Mammel, M. Eppinger, M. J. Rosovitz, D. Wagner, L. Rahalison, J. E. Leclerc, J. M. Hinshaw, L. E. Lindler, T. A. Cebula, E. Carniel, and J. Ravel.** 2007. Multiple antimicrobial resistance in plague: an emerging public health risk. PLoS One **2:**e309.
66. **Welkos, S. L., K. M. Davis, L. M. Pitt, P. L. Worsham, and A. M. Freidlander.** 1995. Studies on the contribution of the F1 capsule-associated plasmid pFra to the virulence of Yersinia pestis. Contrib. Microbiol. Immunol. **13:**299–305.
67. **Wickstrum, J. R., J. M. Skredenske, A. Kolin, D. J. Jin, J. Fang, and S. M. Egan.** 2007. Transcription activation by the DNA-binding domain of the AraC family protein RhaS in the absence of its effector-binding domain. J. Bacteriol. **189:**4984–4993.
68. **Williams, J. E., D. N. Harrison, T. J. Quan, J. L. Mullins, A. M. Barnes, and D. C. Cavanaugh.** 1978. Atypical plague bacilli isolated from rodents, fleas, and man. Am. J. Public Health **68:**262–264.
69. **Winter, C. C., W. B. Cherry, and M. D. Moody.** 1960. An unusual strain of *Pasteurella pestis* isolated from a fatal human case of plague. Bull. W.H.O. **23:**408–409.
70. **Worsham, P. L., and C. Roy.** 2003. Pestoides F, a Yersinia pestis strain lacking plasminogen activator, is virulent by the aerosol route. Adv. Exp. Med. Biol. **529:**129–131.
71. **Wren, B. W.** 2003. The yersiniae—a model genus to study the rapid evolution of bacterial pathogens. Nat. Rev. Microbiol. **1:**55–64.
72. **Zhou, D., Z. Tong, Y. Song, Y. Han, D. Pei, X. Pang, J. Zhai, M. Li, B. Cui, Z. Qi, L. Jin, R. Dai, Z. Du, J. Wang, Z. Guo, J. Wang, P. Huang, and R. Yang.** 2004. Genetics of metabolic variations between Yersinia pestis biovars and the proposal of a new biovar, microtus. J. Bacteriol. **186:**5147–5152.
73. **Zhou, D., and R. Yang.** 2009. Molecular Darwinian evolution of virulence in Yersinia pestis. Infect. Immun. **77:**2242–2250.